OPTOELECTRONICS AND ADVANCED MATERIALS – RAPID COMMUNICATIONS Vol. 2, No. 12, December 2008, p. 798 - 801

Optical properties of $Mg_xZn_{1-x}O$ nanoparticles synthesized by a direct thermal decomposition route

S. LABUAYAI[a], V. PROMARAK[b], S. MAENSIRI[a*]
Department of Physics, Faculty of Science, Khon Kaen University, Khon Kaen, 40002, Thailand
[a]*Integrated Nanotechnology Research Center (INRC), Faculty of Science, Khon Kaen University, Khon Kaen, 40002, Thailand*
[b]*Advanced Organic Materials and Devices Laboratory, Department of Chemistry, Faculty of Science, Ubon Ratchathani University, Varinchamrap, Ubon Ratchathani 34190, Thailand*

$Mg_xZn_{1-x}O$ ($0 \le x \le 0.4$) nanoparticles were synthesized by direct thermal decomposition of Zn and Mg acetates in air at 500 ºC. As revealed by SEM, pure ZnO sample consisted of nanorods, wheras $Mg_xZn_{1-x}O$ samples became nanoparticles. The E_g increased from 3.13 to 3.22 eV with increasing Mg concentration. The PL spectra of all the samples showed a strong UV emission, a weak blue, a weak blue-green, and a weak green bands, indicating their high structure and optical quality.

(Received November 8, 2008; accepted November 27, 2008)

Keywords: Nanoparticles, Zinc oxides, Semiconductors, Thermal decomposition, Optical properties, Photoluminescence

1. Introduction

Zinc oxide (ZnO) is an excellent electronic and photonic material having a wide band gab semiconductors ($E_g \approx 3.27$ eV) and a large exciton binding energy of 60 meV. Therefore, ZnO is attracting considerable attention as one of the important candidates for potential applications including gas sensors, photodetectors, light-emitting diodes, varistors, piezoelectricity [1-5]. Recently, $Mg_xZn_{1-x}O$ materials have attracted much attention because of their wider band gap compared to pure ZnO and their unique UV-luminescent properties based on radiative recombination of electron-hole pairs [6]. Magnesium oxide (MgO), with a wide band gab of 7.7 eV has high transmission in the ultraviolet region. Changing the band gab can be achieved by doping the magnesium in ZnO. So far, a variety of techniques have been applied to the preparation of $Mg_xZn_{1-x}O$, including electrophoresis deposition [7], sol-gel [8], pulsed laser deposition [9], and molecular beam epitaxy [10, 11]. However, these methods involve a strictly controlled synthesis environment, expensive equipments and complicated procedures.

In the present work, we report the optical properties of $Mg_xZn_{1-x}O$ nanoparticles prepared by a direct thermal decomposition of Zn and Mg acetates in air at 500 ºC for 4 h. This method is fast, simple, and cost-effective for synthesis of $Mg_xZn_{1-x}O$ nanoparticles. The structure and morphology of synthesized nanocrystallline $Mg_xZn_{1-x}O$ were characterized by XRD and SEM. Optical properties of the prepared samples were investigated by UV-VIS and photoluminescence spectroscopies.

2. Experimental

For the synthesis of $Mg_xZn_{1-x}O$ nanopartciles, $Zn(CH_3OO)_2.2H_2O$ (≥ 99.5 % Purity, Anala R), and $C_4H_6MgO_4.4H_2O$ (≥ 99.0 % Purity, Fluka) were mixed using a mortar and pestle for several minutes until homogeneous mixture powder was obtained. For each sample, the mole ratio of Mg: Zn was kept corresponding to the nominal composition of $Mg_xZn_{1-x}O$ (x = 0, 0.1, 0.2, 0.3 and 0.4). The mixed powder was then placed in an alumina crucible covered by alumina lid before loading it into oven, and was calcined in air at 500 ºC for 4 h. The calcined samples were analyzed by means of X-ray diffraction (XRD) using CuK_α radiation with $\lambda = 0.15418$ nm (Phillips PW3040, The Netherlands), and UV-VIS-NIR scanning spectroscopy (UV-3101PC, Shimadzu). The particle size and external morphology of the fine calcined samples were characterized by scanning electron microscopy (SEM) (LEO 1450VP, U.K.). Photoluminescence (PL) measurement was carried out on a luminescence spectrometer (Perkin–Elmer LS-55B, PerkinElmer Instrument, USA) using a Xenon lamp as the excitation source at room temperature. The samples were dispersed in dichloromethane and the excitation wavelength used in PL measurement was 325 nm.

3. Results and discussion

XRD patterns of all the samples in Fig. 1 show exactly the same peak patterns, which can be indexed as the ZnO wurtzite structure in the standard data (JCPDS,

36-1451). However, the presence of the second phase as MgO (JCPDS, 45-0946) was observed with Mg concentrations of x ≥ 0.2. The crystal sizes of the prepared samples were estimated from X-ray line broadening using Scherrer's equation (i.e. $D = 0.89\lambda/(\beta\cos\theta)$, where λ is the wavelength of the X-ray radiation, θ is the diffraction angle and β is the full width at half maximum (*FWHM*) [12], and were obtained to be 36.80 ± 2.74 nm, 32.70 ± 4.99 nm, 30.60 ± 4.63 nm, 28.43 ± 4.02 nm and 27.23 ± 3.87 nm for x = 0, 0.1, 0.2, 0.3 and 0.4, respectively. The wurtzite structure lattice parameters *a* and *c* calculated from the XRD spectra are (*a* = 0.32443, *c* = 0.51979), (*a* = 0.32427, *c* = 0.51941), (*a* =0.32423, *c* = 0.51922), (*a* =0.32424, *c* = 0.51915) and (*a* =0.32416, *c* = 0.51899) nm for x = 0, 0.1, 0.2, 0.3 and 0.4, respectively. These values are close to those of lattice *a* = 0.32488 nm and *c* = 0.52066 nm in the standard data (JCPDS, 36-1451). The crystallite size and wurtzite structure lattice parameters *a* and *c* of the samples whose Mg concentration x is from 0 to 0.4 have a decrease on increasing the Mg concentration as reported previously by other research groups [13, 14]. These results indicate that the effective ionic radius (0.57 Å) of Mg^{2+} is smaller than that of Zn^{2+} (0.60 Å) [15].

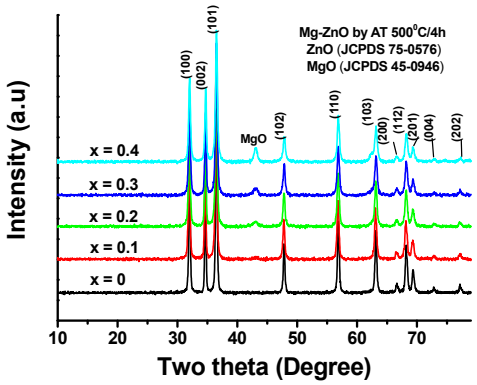

Fig. 1. XRD patterns of the $Mg_xZn_{1-x}O$ nanoparticles prepared in air at 500 °C for 4 h.

The morphology and structure of samples were investigated by SEM (Fig. 2). It is clearly seen from the SEM micrographs that the morphology of samples was affected by the amount Mg concentration. The pure ZnO consisted of nanorods of ~ 60-100 nm in diameter with 200-400 nm in length. Interestingly, the $Mg_xZn_{1-x}O$ (x ≥ 0.1) samples consisted of nanoparticles with particles size of ~ 20-50 nm. This phenomenon is probably due to the affect of impurity (NaCl-type) MgO phase.

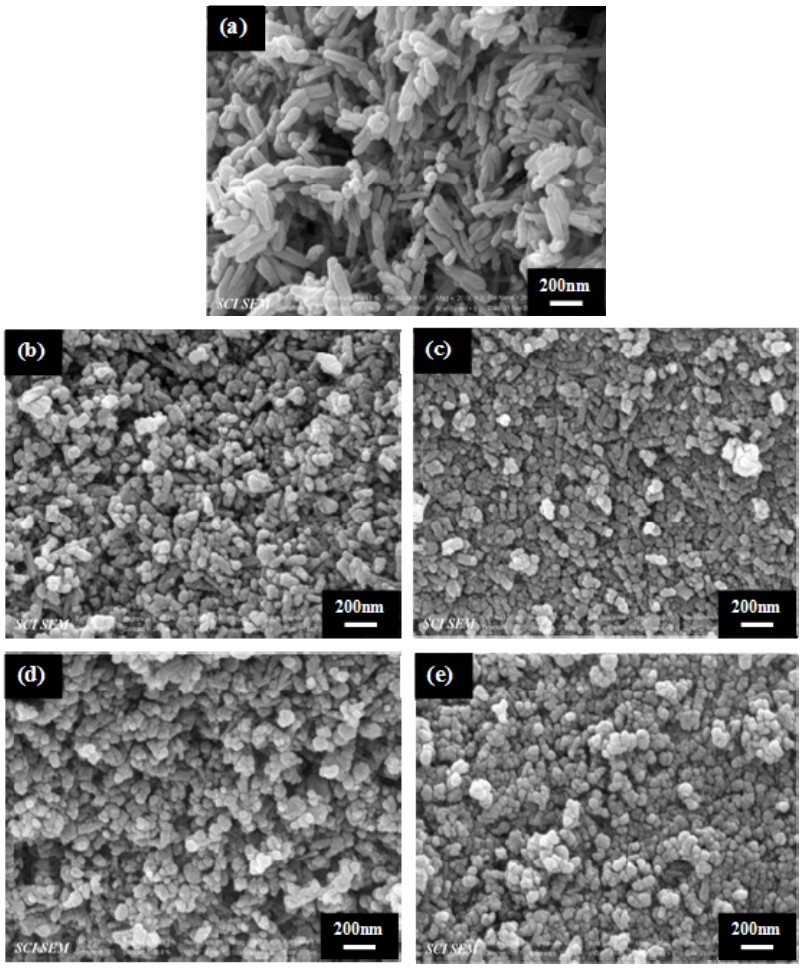

Fig. 2. SEM micrographs of the $Mg_xZn_{1-x}O$ nanoparticles prepared in air at 500 °C for 4 h. (a) x = 0, (b) x = 0.1, (c) x = 0.2, (d) x = 0.3, and (e) x = 0.4.

The UV-visible absorption spectra of all samples shown in Figure 3, exhibited a strong absorption below 400 nm (3.10 eV) with a well defined absorbance peak at around 364 nm (3.41 eV) and 288 nm (4.31 eV). Inset of Fig. 3 shows the calculated band gap energies for different Mg concentration. The band gap energy increased from 3.13 to 3.22 eV with increasing in Mg concentrations from x = 0 to x =0.4. These values are lower than that the Mg-doped ZnO reported in the literature [13, 14, 16]. However, we expect that the wide band gap of MgO (7.7 eV) may be responsible for the increase of the band gap in our $Mg_xZn_{1-x}O$ samples.

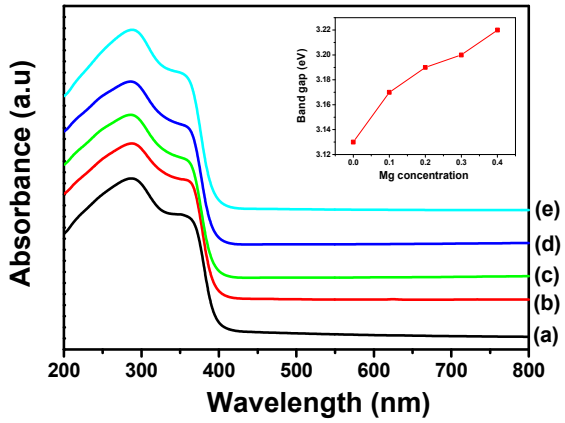

Fig. 3. Room temperature optical absorbance spectra of the $Mg_xZn_{1-x}O$ nanoparticles with (a) x = 0, (b) x = 0.1, (c) x = 0.2, (d) x = 0.3, and (e) x = 0.4. Inset is a plot of band gab energy as a function of Mg concentration (x) for the $Mg_xZn_{1-x}O$ nanoparticles.

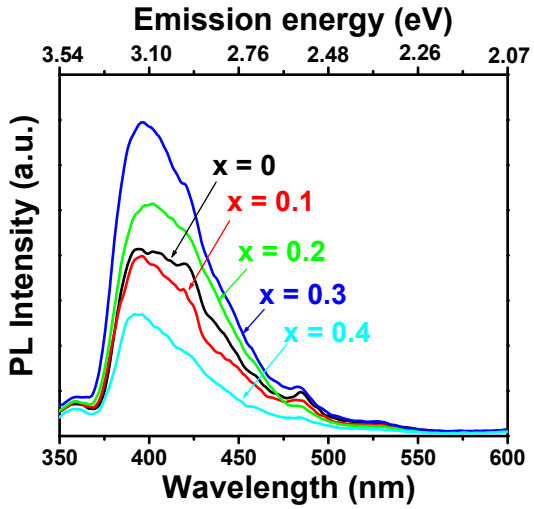

Fig. 4. Room temperature photoluminescence spectra of the synthesized $Mg_xZn_{1-x}O$ samples. The samples were dispersed in dichloromethane and the excitation wavelength used in PL measurement was 325 nm.

Room temperature PL spectra of the nanocrystalline $Mg_xZn_{1-x}O$ samples measured using a Xenon laser of 325 nm as an excitation source are shown in Fig. 4. The spectra of all samples consist of four emission band: a strong UV emission band at ~ 395 nm (3.14 eV), a weak blue band at ~ 420 nm (2.95 eV), a weak blue-green band at ~ 485 nm (2.56 eV), and a very weak green band at ~ 530 nm (2.34 eV). The strong UV emission corresponds to the exciton recombination related near-band edge emission of ZnO [17, 18]. The weak blue and weak blue-green emissions are possibly due to surface defect in the ZnO samples [19-22]. The weak green band emission corresponds to the singly ionized oxygen vacancy in ZnO, and this emission is resulted from the recombination of a photo-generated hole with the singly ionized charge state of the specific defect [23-25]. The low intensity of the green emission may be due to the low density of oxygen vacancies during the preparation of the $Mg_xZn_{1-x}O$ samples, whereas the strong room temperature UV emission intensity should be attributed to the high purity with perfect crystallinity of the synthesized $Mg_xZn_{1-x}O$ samples.

4. Conclusions

$Mg_xZn_{1-x}O$ nanoparticles were prepared by a direct thermal decomposition using Zn and Mg acetates as precursors. The results revealed that the morphology of the prepared $Mg_xZn_{1-x}O$ samples was affected by amount of Mg, causing formations of nanorods for pure ZnO and nanopaticles for Mg-doped ZnO. The band gap of $Mg_xZn_{1-x}O$ samples also increased with increasing Mg concentration. Photoluminescence spectra of all the samples showed four main emission bands including a strong UV emission band, a weak blue band, a weak blue-green band, and a weak green band at 3.14 eV, 2.95 eV, 2.56 eV and 2.34 eV, respectively. The strongest emission spectrum is found for the $Mg_xZn_{1-x}O$ (x = 0.3) sample, suggesting its better crystallinity and optical properties than those of the other samples. This work demonstrates the simple synthesis of $Mg_xZn_{1-x}O$ nanoparticles with good crystallinity and optical properties by a direct thermal decomposition of acetates at low temperature. The current simple synthesis method using cheap precursors can be extended to prepare nanoparticles of other interesting metal oxide materials.

Acknowledgements

The authors would like to thank the Department of Chemistry for providing UV-vis facilities and the Science and the Department of Physics, Ubon Ratchathani University for providing XRD facilities. This work is supported by the "Industry/University Cooperative Research Center (I/UCRC) in HDD Component, the Faculty of Engineering, Khon Kaen University and

National Electronics and Computer Technology Center, National Science and Technology Development Agency".

References

[1] H. W. Lehman, R. Widmer, J. Appl. Phys. **44**, 3868 (1973).
[2] S. Liang, H. Sheng, Y. Liu, Z. Hio, Y. Lu, H. Shen, J. Cryst. Growth. **225**, 110 (2001).
[3] N. Saito, H. Haneda, T. Sekiguchi, N. Ohashi, I. Sakagushi, K. Koumoto, Adv. Mater. **14**, 418 (2002).
[4] E. Olsson, G. Dunlop, J. Am. Ceram. Soc. **76**, 65 (1993).
[5] Z. L. Wang, J. H. Song, Science. **312**, 242 (2006).
[6] T. Makino, K. Tamura, C. H. Chia, Y. Segawa, M, Kawasaki, A. Ohtomo, H. Koinuma, Appl. Phys. Lett. **81**, 2355 (2002).
[7] Y. Jin, B. Zhang, S. Yang, et al., Solid. State. Commun. **119**, 409 (2001).
[8] G. H. Ning, X. P. Zhao, J. Li, Opt. Mater. **27**, 1 (2004).
[9] A. Ohtomo, M. Kawasaki, T. Koida, K. Masubuchi, H. Koimuna, Appl. Phys. Lett. **72**, 3327 (1999).
[10] A. Ohtomo, M. Kawasaki, Y. Sakurai, I. Ohkubo, R. Shiroki, Y. Yoshida, T. Yasuda, Y. Segawa, H. Koinuma, Mater. Sci. Eng. B **56**, 263 (1998).
[11] K. Ogata, K. Koike, T. Tanite, T. Komoro, F. Yan, S. Sasa, M. Inoue, M. Yano, J. Cryst. Growth **251**, 623 (2003).
[12] B. D. Cullity, S.R. Stock, "Elements of X-ray Diffraction", Prentice Hall, New Jersey, 3ed. (2001).
[13] Y. S. Wang, J. Cryst. Growth **304**, 393 (2007).
[14] F. K. Shan, B. I. Kim, G. X. Liu, Z. F. Liu, J. Y. Sohn, W. J. Lee, B. C. Shin, Y. S. Yu, J. Appl. Phys. **95**, 4772 (2004).
[15] R. Shannon, Acta Crystallogr., Sect. A: Cryst. Phys. Diffr. Theor. Gen. Crystallogr. **32**, 751 (1976).
[16] Y. S. Wang, P. J. Thomas, P. O. Brien, J. Phys. Chem. B **110**, 21412 (2006).
[17] K. Vanheusden, W.L. Warren, C.H. Sesger, D.R. Tallant, J.A. Voigt, B.E. Gnage, J. Appl. Phys. **79**, 7983 (1996).
[18] S. C. Lyu, Y. Zhang, H. Ruh, H. Lee, H. Shim, E. Suh, C. J. Lee, Chem. Phys. Lett. **363**, 134 (2002).
[19] J. Wang, L. Gao, Solid State Comm. **132**, 269 (2004).
[20] S. Maensiri, C. P. Laokul, V. Promarak, J. Cryst. Growth **289**, 102 (2006).
[21] K. Pato, E. Swatsitang, W. Jareonboon, S. Maensiri, V. Promarak, Optoelectron. Adv. Mater. Rapid Comm. **1**, 287 (2007).
[22] S. Maensiri, C. Masingboon, V. Promarak, S. Seraphin, Opt. Mater. **29**, 1700 (2007).
[23] Y. Li, G.S. Cheng, L.D. Zhang, J. Mater. Res. **15**, 2305 (2000).
[24] S. Monticone, R. Tufeu, A. V. Kanaev, J. Phys. Chem. B **102**, 2854 (1998).
[25] B. D. Yao, Y. F. Chan, N. Wang, Appl. Phys. Lett. **81**, 757 (2002).

*Corresponding author: sanmae@kku.ac.th
santimaensiri@gmail.com